J. Serb. Chem. Soc. 70 (3) 361–369 (2005)
JSCS –3277

UDC 54–72:535.342:543.48
Original scientific paper

Influence of Mie scattering on nanoparticles with different particle sizes and shapes: photometry and analytical ultracentrifugation with absorption optics

M. D. LECHNER

Physical Chemistry, University of Osnabrueck, 49069 Osnabrueck, Germany
(e-mail: lechner@uni-osnabrueck.de)

(Received 24 November 2004)

Abstract: Nanoparticles are used in large quantities for very different applications. A precise determination of the diameter and the particle size distribution which is responsible for the application properties is therefore essential. Reliable methods for measuring the above mentioned quantities are photometric measurements and analytical ultracentrifugation with an UV optics detector. Both methods are ruled by the Mie effect, that is scattering and absorption of the particles as function of the diameter, the wavelength, and the shape of the particles. The extinction coefficients $\varepsilon = \tau/c$ for spheres, rods, and core shell particles have been calculated and plotted over a wide range of the size parameter $\pi\, d/\lambda$. Two examples for multimodal latex particles and core shell particles have been given and demonstrate the applicability of the method.

Keywords: Mie scattering, analytical ultracentrifugation, absorption optics, particle size, particle size distribution.

INTRODUCTION

Nanoparticles are produced in large quantities for very different applications such as lacquers, dyes, cosmetics, food, magnetic storage materials, catalysts, and print materials. On the other hand, biological systems contain different nanoparticles, *e.g.*, liposomes. An important physical quantity of all nanoparticles is their diameter or, in the case that the nanoparticles consist of different diameters, the particle size distribution. The most reliable experimental methods for the characterization of nanoparticles are photometric measurements, analytical ultracentrifugation (AUC), and dynamic light scattering (DLS). AUC has the advantage that the particles are fractionated during sedimentation, therefore, different sizes of particles may be detected with high precision, *i.e.*, the complete size distribution at high resolution.

In this paper the extinction coefficient $\varepsilon = \tau/c$ for spheres, rods, and core shell particles have been calculated and plotted over a wide range of the size parameter $\pi d/\lambda$. Subsequently two examples for spheres and core shell particles are presented.

EXTINCTION COEFFICIENT FOR SPHERES, RODS, AND CORE SHELL PARTICLES

If light passes a solution the intensities of the incident and the scattered beam together with the absorbed beam follow Lambert-Beer's law:

$$\ln(I_p/I) = \tau l;\ \tau = \varepsilon c \tag{1}$$

with I_p = intensity of the incident beam, I = intensity of the beam passing the solution, τ = turbidity, l = length of the cell, c = concentration of the particles in the solution and $\varepsilon = \tau/c$ = specific turbidity or extinction coefficient. With this law in mind photometric measurements or analytical ultracentrifuge measurements with absorption optics allow the determination of the particle concentration under the assumption that the extinction coefficient ε could be calculated. Fractionation of the particles in the analytical ultracentrifuge allows the determination of the particle size distribution of the dissolved or dispersed particles.

The calculation of the extinction coefficient for spheres has been done by Mie.[1] Starting with Maxwell's equations Mie has developed the extinction efficiency Q_{ext} as a function of the size parameter $\pi\, d/\lambda$ (d = diameter, $\lambda = \lambda_0 / n_0$ = wavelength) and the refractive indices of the solvent n_0 and the spherical particles n_1. In the case that the incident light is not only scattered but also absorbed by the particle the complex refractive index of the particle $N_1 = n_1 + ik_1$ with $i = (-1)^{1/2}$ has to be applied. The complete equations for Q_{ext} are found in the literature[1–5]. For the extinction cross section c_{ext} (total light energy absorbed and scattered by one sphere) it holds:

$$c_{ext} = Q_{ext}\, \pi\, d^2 / 4 \tag{2}$$

The turbidity or attenuation coefficient τ is then definied as

$$\tau = {}^1N\, c_{ext} \tag{3}$$

with ${}^1N$ = number of particles per unit volume (particle number density). Conversion of ${}^1N$ to $\varphi = {}^1N\, v$ with φ = volume fraction of the particles in the collection and $v = (1/6)\, \pi\, d^3$ = volume of a single particle yields

$$\tau = \varphi\, c_{ext}/v \tag{4}$$

Combination of Eqs. (2) – (4) yields

$$\tau = \varphi\, Q_{ext}\, \pi\, d^2\, 6 / (4\, \pi\, d^3) = \varphi\, Q_{ext}\, 3 / (2\, d) \tag{5}$$

In many cases the mass concentration $c = m_1 / V$ (m_1 = mass of the particles and V = volume of the solution) instead of the volume fraction of the particles is

preferred. As $\varphi = V_1/(V_0 + V_1) \approx m_1\,(\rho_1\,V_0) = c/\rho_1$ (ρ_1 = density of the particles) the final equations for the turbidity τ and the specific turbidity $\varepsilon = \tau/c$ for spheres are obtained:

$$\tau = c\,Q_{\text{ext}}\,3\,/\,(2\,d\,\rho_1);\ \tau\,/\,c = \varepsilon = Q_{\text{ext}}\,3\,/\,(2\,d\,\rho_1);\ \text{(spheres)} \qquad (6)$$

In the cases of scientific and technical applications coated spheres are of major interest. Examples are liposomes and grafted polymer particles which are widely used in industry.

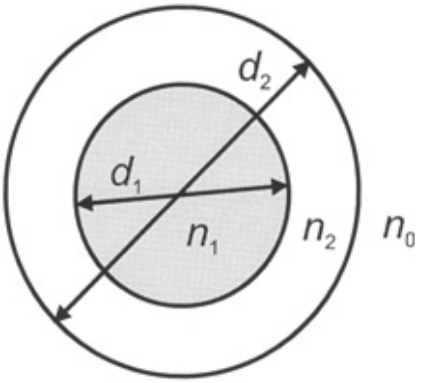

Fig. 1. Dimensions and notation of a coated sphere.

In Fig. 1 n_0, n_1, and n_2 are the refractive indices of the medium, the core and the shell, respectively and d_1 and d_2 are the diameters of the core and the shell. The values of Q_{ext} as functions of n_0, n_1, n_2, d_1, d_2 and λ are given in the literature.[2,3,6,7]

Figures 2a and 2b demonstrate the specific turbidity τ/c as a function of the reduced size parameter $\pi\,d/\lambda$ for spheres. The τ/c values were calculated according to Eq. (6) with $\rho_1 = 1$ g/cm^3. For densities of the particles which differ from unity one has to divide the τ/c values with ρ_1. The lower diameter scale refers to a wavelength $\lambda_0 = 546.1$ nm and a refractive index of the solvent of $n_0 = 1.333$. The figures show, that Mie's theory includes the Rayleigh scattering of small molecules with diameters down to 1 nm. As has been shown by Dezelic and Kratohvil[8] the theories of Rayleigh and Mie are nearly indentical with respect to the specific turbidity in the range $0 < \pi\,d/\lambda < 0.3$. The figures indicate the angle independent Rayleigh scattering ($d < \lambda/20$), the angle dependent Rayleigh scattering ($\lambda > d > \lambda/20$) and the Mie scattering ($d > \lambda$).

Figure 3 compares the specific turbidity τ/c of coated spheres with different values for n_1/n_0 for $n_2/n_0 = 1.10$ and $d_1 = (d_2 - 40)$ [nm]; one curve has been calculated with $k_1 = 0.02$ (k_1 is the imaginary part of the refractive index). Dependent on the different diameters and the refractive indices the differences with respect to non-coated spheres are remarkable. Coated spheres with constant thickness of the coat are typical for grafted polymer particles and liposomes.

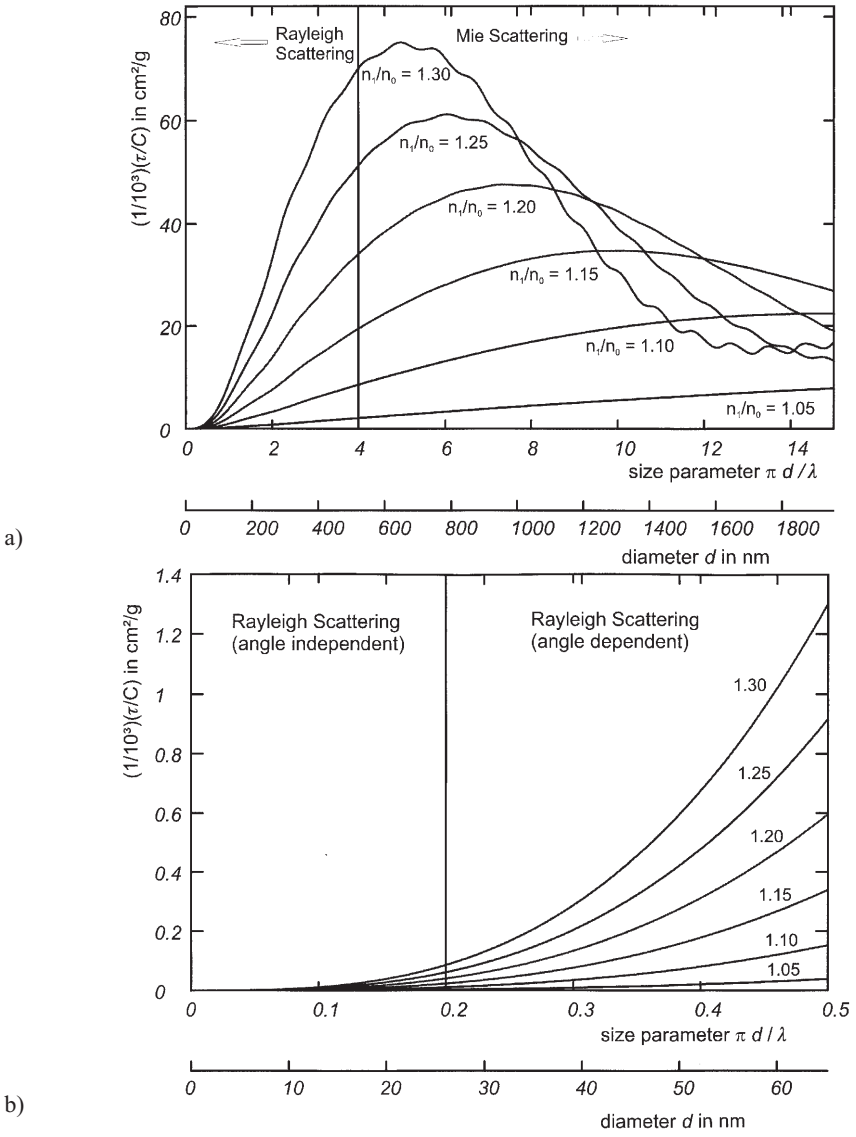

Fig. 2. Specific turbidity $\varepsilon = \tau/c$ for spheres as a function of the size parameter $\pi\, d/\lambda$ for different relations of the refractive indices n_1/n_0: (a) for $0 < \pi d/\lambda < 15$; (b) for $0 < \pi d/\lambda < 0.5$. The lower diameter axis d refers to $\lambda_0 = 546.1$ nm and $n_0 = 1.333$.

Regarding cylinders with infinite length and diameter d, similar equations according to that of a sphere are obtained:[2–4,9,10]

$$\tau/c = \varepsilon = Q_{\text{ext}}\, \pi / (d\, \rho_1); \text{ (cylinders)} \tag{7}$$

Figures 4a and 4b show the specific turbidity τ/c for cylinders with infinite

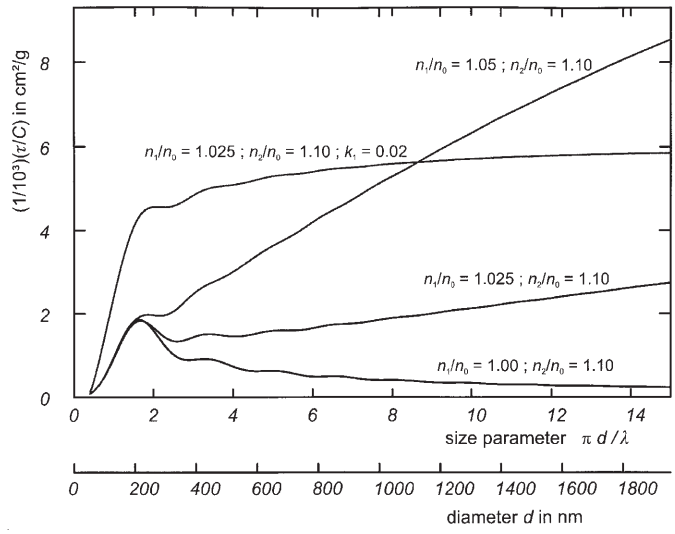

Fig. 3. Specific turbidity $\varepsilon = \tau/c$ for coated spheres as a function of the size parameter $\pi\, d/\lambda$ for different relations of the refractive indices n_1/n_0, for $0 < \pi d/\lambda < 15$, for $n_2/n_0 = 1.10$ and $d_1 = (d_2 - 40)$ [nm]; one curve has been calculated with $k_1 = 0.02$ (absorption). The lower diameter axis d refers to $\lambda_0 = 546.1$ nm and $n_0 = 1.333$.

length and diameter d. The calculations are done in the same way as for spheres and coated spheres. The extinction efficiency Q_{ext} is given in the literature.[2–5] As the calculation is done for cylinders with infinite length, the experimental results fit best the theoretical values for sufficiently large l/d values (l is the length of the cylinder). Figures 4a and 4b demonstrate remarkable differences between spheres and cylinders with respect to the specific turbidity.

The calculation of $\varepsilon = \tau/c$ in conjunction with Lambert–Beer's law, Eq. (1) enables the determination of the concentration of the particles c if the optical density $\ln(I_p / I)$ and the thickness of the solution in a cuvette could be measured. Fractionation of the particles by applying a gravitational field allows the determination of the particle size distribution.

In principle there are two possibilities for the measurement of the particle size distribution with an analytical ultracentrifuge:

a) The AUC has a variable slit moving as fast as possible during distinct times from the meniscus to the bottom. A lamp illuminating the slit together with a light detector measures the intensity $I(t)$ as a function of the rotor distance r. This method may be improved by positioning many light detectors, *i.e.*, photodiodes along the complete distance from the meniscus r_m to the bottom r_b.

b) The AUC has a constant slit with a radius position $r_s \approx (r_m + r_b)/2$. A lamp illuminating the slit together with a light detector measures the intensity $I(t)$ of the moving particles at a constant rotor distance r_s. Most of the AUC techniques for the

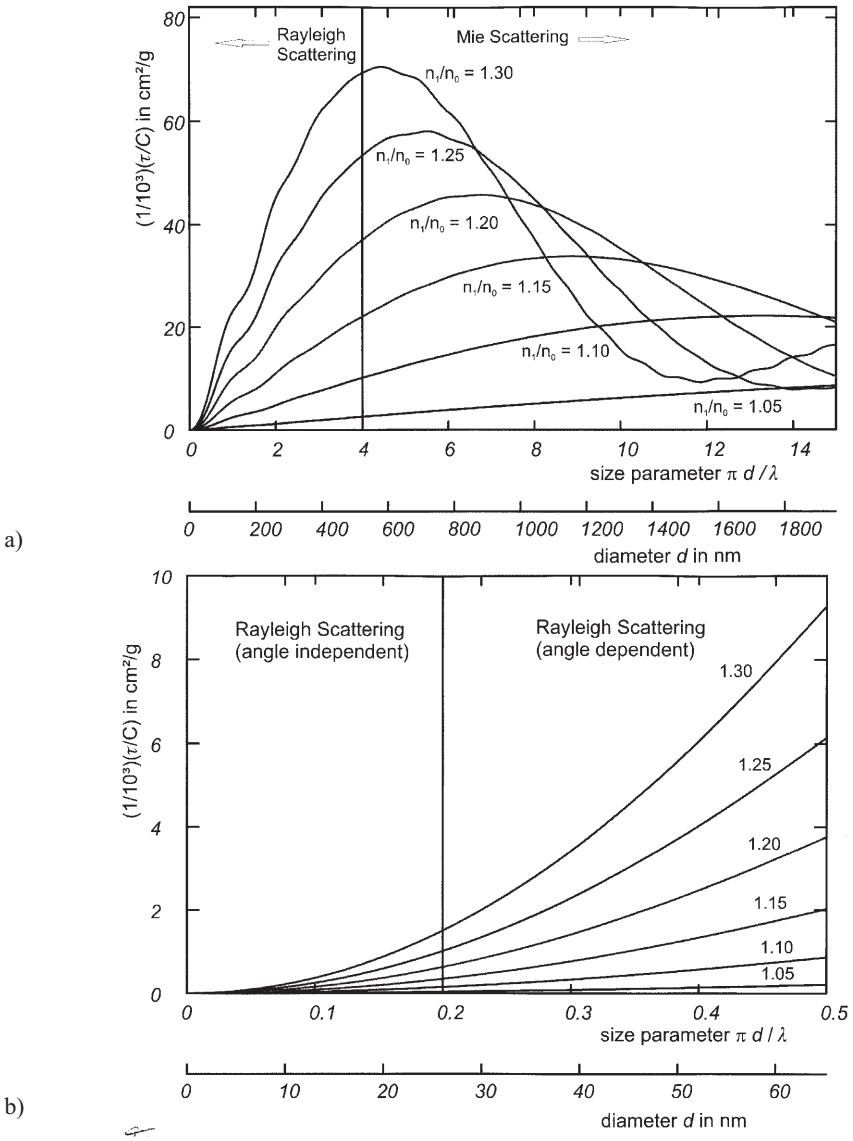

Fig. 4. Specific turbidity $\varepsilon = \tau/c$ for cylinders as a function of the size parameter $\pi\, d/\lambda$ for different relations of the refractive indices n_1/n_0: (a) for $0 < \pi d/\lambda < 15$; (b) for $0 < \pi d/\lambda < 0.5$. The lower diameter axis d refers to $\lambda_0 = 546.1$ nm and $n_0 = 1.333$.

determination of the particle size distribution use this second method. The following equations hold for this method.

Following Eq. (1) the ratio of the turbidity at the time t, $\tau(t)$ and the turbidity at the time $t = 0$, $\tau(0)$ could be determined *via* the experimentally accessible intensities of the solution and the solvent:

$$\tau(t)\tau(0) = \{\ln[I(t)/I_p]\}/\{\ln[I(0)/I_p]\} \quad (8)$$

with $I(t)$ and $I(0)$ = intensities of the solution at the time t and at the time $t = 0$, respectively, and I_p = intensity of the solvent. In the case that all dissolved or dispersed particles have identical specific turbidites $\varepsilon_i = \varepsilon$ the relative concentration of the particles could easily be determined:

$$\tau(t)\tau(0) = c(t)/c(0) = W(d) \quad (9)$$

Using an analytical ultracentrifuge particles with different sizes could be fractionated according to their diameter using Stoke's well known law:[11]

$$d_i^2 = 18\,\eta_{slv}\,S_i/(\rho_{sol} - \rho_{slv})\;;\; S_i = [\ln(r_s/r_h)]/\int \omega^2 \mathrm{d}t \quad (10)$$

with d_i = diameter of the species i, η_{slv} = viscosity of the solvent, S_i = sedimentation coefficient of the species i, ρ_{sol} = density of the solute, ρ_{slv} = density of the solvent, r_s = radius position of the slit in the ultracentrifuge cell, $r_h = r_m$ = radius position of the meniscus in the cell in the case of sedimentation of the particles, $r_h = r_b$ = radius position of the bottom in the cell in the case of flotation of the particles, and ω = angular velocity of the rotor.

For sector shaped cells the dilution rule has to be applied:

$$c_i(t)/c_i(0) = (r_h/r_s)^2 \quad (11)$$

In the case of different particle sizes one has to apply for each species a different specific turbidity $(\tau/c)_i = \varepsilon_i$ according to Eqs. (6) and (7):

$$\tau(t)/\tau(0) = \sum_{i=1}^{N} \tau_i(t) / \tau(0) = (1/\varepsilon_0)\sum_{i=1}^{N} \varepsilon_i c_i(t) / c(0) \quad (12)$$

with $i = 1, 2, ..., N$ being the species number.

EXPERIMENTAL

The experimental setup has been described extensively in the literature.[12] Several monodisperse polystyrene calibration latices with different diameters have been produced by BASF AG, Ludwigshafen. The core-shell particle has been synthesized by emulsion polymerization of styrene with subsequent grafting of the particles with methyl methacrylate. The particles were dispersed in water with 0.5 % of a surfactant.

RESULTS AND DISCUSION

Figure 5 shows AUC measurements on a polystyrene latex mixture (the polystyrene latices were synthesized by BASF AG, Ludwigshafen, Germany) with diameters 200, 350, 520, 700, 950 and 1450 nm. Curve A is the integral particle size distribution of the latex mixture without Mie correction; curve B is the Mie corrected integral distribution. The differences are dramatical. It has been demonstrated that the Mie correction has a large influence on the size distribution of the particles. The differential curve is the derivation of the Mie corrected curve B.

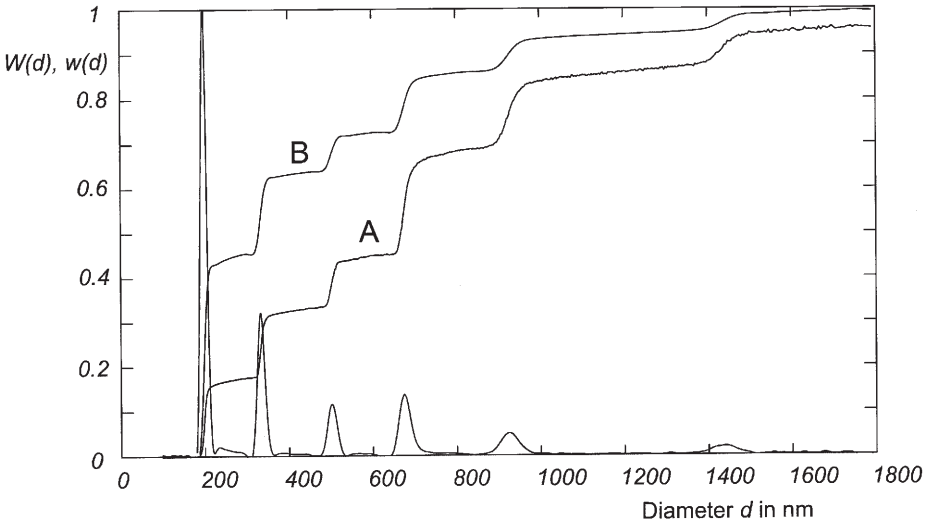

Fig. 5. AUC measurements on a polystyrene latex mixture with diameters 200, 350, 520, 700, 950 and 1450 nm. Curve A: integral particle size distribution of the latex mixture without Mie correction. Curve B: Mie corrected integral distribution. Differential curve: derivation of curve B.

Figure 6 shows AUC measurements on a core shell particle with a polystyrene core and a poly(methyl methacrylate) shell. The refractive indices of the core were assumed as $n = 1.60$ and that of the shell as $n = 1.50$; the thickness of the shell was assumed to be 40 nm. Curve A is the integral particle size distribution of the core shell particle without Mie correction; curve B is the Mie corrected integral distribution. The

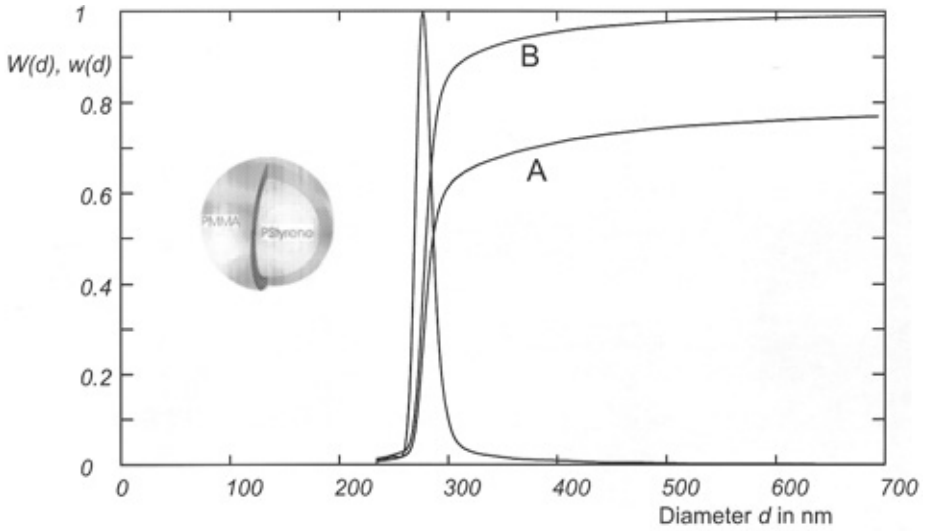

Fig. 6. AUC measurements on a core shell particle with a polystyrene core and a poly(methyl methacrylate) shell (see text).

differential curve is the derivation of the Mie corrected curve B. The result of the evaluaton was that the production of this core shell particle was performed without side reactions and a remarkable narrow distributed size particle distribution.

Acknowledgement. This work was supported by BASF AG, Ludwigshafen, Germany. The author is thankful to Dr. L. Börger, BASF AG for helpful discussions and M. Stadler, BASF AG for performing the measurements.

ИЗВОД

УТИЦАЈ МИЈЕВОГ РАСИПАЊА НА НАНОЧЕСТИЦЕ РАЗЛИЧИТИХ ВЕЛИЧИНА И ОБЛИКА: ФОТОМЕТРИЈА И АНАЛИТИЧКО УЛТРАЦЕНТРИФУГИРАЊЕ СА АПСОРПЦИОНОМ ОПТИКОМ

M. D. LECHNER

Physical Chemistry, University of Osnabrueck, 49069 Osnabrueck, Germany

Наночестице се користе у великим количинама за веома различите сврхе. Прецизно одређивање пречника наночестица, као и расподеле величина ових честица је од суштинске важности, будући да су то карактеристике одговорне за њихова својства која су битна за примену. Поуздане методе одређивања претходно поменутих величина су фотометријска мерења и аналитичко ултрацентрифугирање са UV оптичким детектором. Обе ове методе су засноване на Мијевом ефекту, тј. на расипању и апсорпцији светлости од стране честица као функције пречника, таласне дужине и облика честица. Коефицијенти екстинкције, $\varepsilon = \tau/c$, за сфере, штапиће и сферне честице са језгром и омотачем су израчунати и графички представљени у функцији од параметра величине честица, $\pi d/\lambda$, у широком опсегу његових вредности. Дата су два примера мултимодалних честица латекса и сферних честица са језгром и омотачем и приказана је применљивост ове методе.

(Примљено 24. новембра 2004)

REFERENCES

1. G. Mie, *Ann. Phys.* **25** (1908) 377
2. M. Kerker, *The Scattering of Light and other Electromagnetic Radiation*, Academic Press, New York, 1969
3. C. F. Bohren, D. R. Huffman, *Absorption and Scattering of Light by Small Particles,* Wiley, New York, 1983
4. P. W. Barber, S. C. Hill, *Light Scattering by Particles: Computational Methods*, World Scientific, Singapore, 1990
5. W. Heller, W. J. Pangonis, *J. Chem. Phys.* **26** (1957) 498
6. A. L. Aden, M. Kerker, *J. Appl. Phys.* **22** (1951) 1242
7. R. W. Fenn, H. Oser, *Appl. Opt.* **4** (1965) 1504
8. G. Dezelic, J. P. Kratohvil, *Kolloid-Z.* **173** (1960) 38
9. B. Larkin, S. W. Churchill, *J. Opt. Soc. Am.* **49** (1959) 188
10. A. C. Lind, J. M. Greenberg, *J. Appl. Phys.* **37** (1966) 3195
11. W. Scholtan, H. Lange, *Kolloid-Z. u. Z. Polym*. **250** (1972) 782
12. W. Mächtle, *Biophys. J.* **76** (1999) 1080.